Middle East Journal of Applied Sciences
Volume: 14 | Issue: 03| July – Sept. | 2024

EISSN: 2706 -7947 ISSN: 2077- 4613
DOI: 10.36632/mejas/2024.14.3.42
Journal homepage: www.curresweb.com
Pages: 559-580

The Biological Efficiency of Gold *Bauhinia variegata* Nano-Extract and Its Impact On the Brains of Diabetic Rats

Amal G. Hussien and Nagwa I. Omar

Biochemistry Department, Biotechnology Research Institute, National Research Centre, 33 El Bohouth St., Dokki 12622, Giza, Egypt

Received: 05 August 2024 **Accepted:** 10 Sept. 2024 **Published:** 20 Sept. 2024

ABSTRACT

The objective of this research was to reveal the biological efficacy of *Bauhinia variegata* extract incorporated with gold nanoparticles (Au-NPs) in preventing adverse effects on the brain of diabetic rats. Total antioxidant capacity level (TAC), peroxidation products concentration, acetylcholine esterase (ACHE) and β-amyloid (Aβ) levels, interleukin-1β (IL-1β) level and tumor necrosis factor-α (TNF-α) level were assayed in brain tissues. Furthermore, different native protein and isoenzyme patterns. The findings of this study demonstrated that normal and diabetic rats received gold *B. variegata* nano-extract showed a significant decrease in TAC level with increasing peroxidation products concentration, ACHE and Aβ levels as well as elevation in the levels of TNF-α and IL-1β. Native electrophoretic protein and isoenzyme patterns showed that administration of gold nano-extract caused physiological alterations. Compared to the similarity index (SI) in the brains of control rats, the severity of physiological alterations increased more in the diabetic group treated with nano-extract than in the diabetic and gold nano-extract treated groups. In conclusion, the native *B. variegata* extract exhibited higher physiological ameliorative effect more than gold nano-extract against the deleterious effects induced in brains of diabetic rats.

Keywords: Diabetes mellitus, *Bauhinia variegata* L., Green Nanotechnology, Electrophoresis, Isoenzymes

1. Introduction

Diabetes mellitus (DM) is categorized as a complex autoimmune metabolic disorder affecting approximately 422 million people globally (Chen *et al*., 2017). It is occurred due to β-pancreatic cells destruction by macrophages and lymphocytes that results in chronic hyperglycemia, insulin resistance, and/or insulin secondary deficiency **(**Xiong *et al*., 2021).

Type 2 diabetes represents approximately 90-95% of all DM cases. It is indicated by blood glucose high levels due to insufficient insulin production by the pancreas. An inflammatory response occurs as a result of the immune response to high blood glucose levels and the presence of inflammatory mediators in fat tissue produced by macrophages and adipocytes. Low and chronic inflammation damages pancreatic β-cells and leads to insufficient insulin production, which results in hyperglycemia (Borai *et al*., 2016; Berbudi *et al*., 2020).

Previous studies have demonstrated that there is an association between DM and numerous brain conditions, such as cerebral ischemia (Liu *et al*., 2022), microangiopathy, macrovascular disease, brain atrophy and cognitive decline **(**EL-Mohandes *et al*., 2023). DM induces morphological, structural and functional brain alterations. Liu *et al.* (2022) reported that the mitochondria-dependent cell death pathway and mitochondrial dysfunction may play important roles in mediating DM with ischemic brain damage. Therefore, brain tissue was selected for the present study.

Corresponding Author: Amal Gouda Hussien, Biochemistry Department, Biotechnology Research Institute, National Research Centre, 33 El-Bohouth St., Dokki 12622, Giza, Egypt
E-mail: amalgouda2022@gmail.com

Traditional therapies originated from plant-derived herbal sources with anti-diabetic activity showed a vital role in controlling DM (Mahomoodally *et al*., 2021). *Bauhinia variegata* L. (*B. variegata*) belongs to the family *Fabaceae* that used in traditional medicine, especially in India. It is characterized by various biological activities such as antimicrobial, antitumor, anti-diabetic, anti-inflammatory diuretic and analgesic effects **(**Hago *et al*., 2021). Glycosides, flavonoids, steroids and terpenes are considered the most active phytoconstituents exist widely in different parts of *B. variegata* in addition to the presence of isoquercetin, quercetin 3-methyl ether, naringenin, rutin and luteolin in plant leaves (Kulkarni and Garud, 2016; Kamal *et al*., 2022). Furthermore, the ethanolic extract of *B. variegata* leaves is rich in insulin-like protein that with an amino acid sequence partially identical to that of bovine insulin, which effectively lowers blood glucose levels **(**Rashid, 2014). Many populations of the world used the leaves of many Bauhinia species in antidiabetic treatments (Hago *et al*., 2021; Mahomoodally *et al*., 2021). Stem bark is used in India in the Ayurvedic system of medicine as an antidiabetic **(**Rashid, 2014). In an *in-vitro* study, the *B. variegata* ethanolic extract and its major constituent, roseoside, have demonstrated enhanced insulin release from the beta-cell lines INS-1(Rashid, 2014; Hago *et al*., 2021). In view of these facts, this work studied the influence of the leaves extract of *B. variegata* on Streptozotocin (STZ) induced hyperglycemia in rats.

Most bioactive compounds have large molecular weight, which affects their absorption through cellular membranes and decreases their bioavailability and efficiency. Nanotechnology is used to solve such problems, by increasing their efficiency, stability, bioavailability, and solubility; decreasing their toxicity and achieving their release to the appropriate site of action **(**Mamillapalli *et al*., 2016). Therefore, incorporating metal nanoparticles (M-NPs) into plant extracts may be one of the most promising solutions to overcome various problems, as poor solubility, distribution, and absorption properties of organic compounds **(**Khandanlou *et al*., 2020). This was supported by a number of recent studies in which silver nanoparticles (Ag-NPs) were incorporated into *Croton tiglium* seeds **(**Aboulthana *et al*., 2020) and *Moringa oleifera* leaf extracts (Aboulthana *et al*., 2021) to be used against colon cancer in rats. Also, gold nanoparticles (Au-NPs) incorporated to *B. variegata* leaves extracts have been used to treat diabetes mellitus **(**Abdel-Halim *et al*., 2020). In 2022, Aboulthana *et al.* emphasized that *Portulaca oleracea* leaves extracts showed higher hepatoprotective effect when incorporated with zinc oxide nanoparticles (ZnO-NPs). Our study was intended to appraise the efficacy of *B. variegata* extract before and after Au-NPs incorporation on the deleterious effects of Streptozotocin (STZ) on the brains of diabetic rats.

2. Materials and Methods

Chemicals

All chemicals including Streptozotocin (STZ), Coomassie brilliant blue G-250, Sudan Black B (SBB), Benzidine, Potassium Iodide, α and β-Naphthyl Acetate were purchased from Sigma-Aldrich (St. Louis, MO, USA).

Gold nano-extract Preparation and Administration

Fresh leaves of *Bauhinia variegata* [(genus *Bauhinia*), collected from El-Orman garden (Giza, Egypt)] were identified by Mrs. Trease Labib (a Plant Taxonomy Consultant at the Egyptian Ministry of Agriculture and Land Reclamation). A voucher specimen was deposited in the Herbarium of the National Research Centre (CAIRC), Giza, Egypt by prof. Dr. Mona M. Marzouk. The extraction was carried out according to the method described by Abdel-Halim *et al.* (2020). *In vitro,* according to the total antioxidant capacity, total polyphenolic compounds, total reducing power and radical scavenging properties of *B. variegata* extracts obtained using different solvents (methanol, ethanol, water and ethyl acetate) by Abdel-Halim *et al.* (2020), the ethanolic extract of *B. variegata* was found to be the most effective extract; thus, it was selected for incorporation with Au-NPs according to the methods of Elia *et al.* (2014). Consequently, the biosynthesized Au-NPs characterization was performed by X-ray diffraction (XRD) and transmission electron microscopy (TEM).

Based on our previous findings, the median lethal dose (LD_{50}) of the native extract of *B. variegata* and gold nano-extract were 36.50 and 51.5 ml/kg, respectively, and their therapeutic doses (1/20 LD_{50}) were 1.83 and 2.58 ml/kg, respectively **(**Abdel-Halim *et al.*, 2020).

Experimental Design

Thirty-six (36) healthy Western albino male rats (150-180 g) were housed for one week in the Animal House, National Research Centre, Dokki, Giza, Egypt for acclimation. Rats had free access to food and water; and were maintained under normal environmental and nutritional conditions. Rats were divided randomly into 6 groups (6 rats per group) as follows:

Group 1: Normal rats were provided a normal diet and tap water (Control group, C). **Group 2:** rats were orally administered the ethanolic extract of *B. variegata* (1.83 ml/kg) for four weeks (extract gp). **Group 3:** rats were administrated gold nano-extract orally (2.58 ml/kg) for four weeks (Nano-extract gp). **Group 4:** rats were intraperitoneally (*i.p*.) injected with STZ (60 mg/kg b.w., single dose) dissolved in citrate buffer (0.1 M, pH 4.5) (Diabetic group) (Sachdewa *et al*., 2001). After 72 h of STZ injection, fasting blood glucose levels were quantified using an Accu-Chek sensor (comfort glucometer, China). Rats with fasting blood glucose level ≥250 mg/dl were considered diabetic. **Group 5:** diabetic rats treated with ethanolic *B. variegata* extract for four weeks (Diabetic + native *B. variegata* extract group). **Group 6:** diabetic rats treated with gold *B. variegata* nano-extract for four weeks (Diabetic + gold *B. variegata* nano-extract group).

Collection of Samples

After 4 weeks, rats were fasted after the last dose of treatment for 18 hr and were injected intraperitoneally with a combination of tiletamine (25 mg/kg) and zolazepam (25 mg/kg) together with xylazine (5 mg/kg) for euthanasia. Consequently, the brain tissues were excised and divided into 2 portions. Portion I [homogenized using Tissue Master TM125 (Omni International, USA) in potassium phosphate buffer (pH 7.4)], and the homogenate was centrifuged at 3000 rpm for 10 min. The supernatant was collected for biochemical assays and stored at -80^{o}C. Portion II was rapidly frozen in liquid nitrogen for electrophoretic analysis. The animal experiments were certified by the Local Ethics Committee for Animal Care and Use at the National Research Centre, Egypt (Registration number 19070). This study was performed according to (The Animal Research: Reporting of *in vivo* Experiments) ARRIVE guidelines.

Biochemical analyses

Total antioxidant capacity (TAC) (Koracevic *et al*., 2001); lipid peroxidation product (LPO) (Ohkawa *et al*., 1979) and total protein carbonyl content (TPC) (Levine *et al*., 1994) were determined as oxidative stress markers. Brain contents of β-amyloid (Aβ) and brain acetylcholine esterase (ACHE) were assessed by Ray Bio elisa kit (USA) and USCN Life Science elisa kit (china), respectively. Also, Interleukin-1β (IL-1β) according to March *et al*. method (1985) and Tumor Necrosis Factor-α (TNF-α) (Engelmann *et al*., 1990) were determined as markers of inflammatory response.

Statistical Analysis

One-way analysis of variance (ANOVA) followed by Bonferroni Post-Hoc test was performed to estimate significant differences among groups. Data are reported as the means values ± SEs, and differences between groups were considered to be significant at $p \leq 0.05$.

Electrophoretic Patterns

The brain tissues were frozen in liquid nitrogen, ground and homogenized in Tris-HCl buffer (0.01 M, pH 7.4). Then, the homogenates were centrifuged at 4˚C for 15 min at 10,000 rpm. Supernatants that contain water-soluble proteins were relocated to new tubes. Concentration of total protein in all tissue homogenates was determined according to Bradford (1976) using bovine serum albumin as a standard. Total protein concentration should approximately be identical in the samples loaded in all wells.

Native Protein Patterns

According to the methods described by Hames (1990), native proteins were electrophoretically separated [Polyacrylamide Gel Electrophoresis (PAGE)] and recently modified by Darwesh *et al.* (2015), who stated that running buffers, gels and samples lacked sodium dodecyl sulfate. Native bands were visualized via Coomassie Brilliant Blue (G-250). Additionally, lipid and calcium moieties

of native gels were stained by isoelectrophoresis [lipid moiety was stained by Sudan Black B (SBB)] **(**Subramaniam and Chaubal, 1990).

Isoenzyme Patterns

After electrophoretic run, the native gels were stained for the electrophoretic detection of catalase (CAT) **(**Siciliano and Shaw, 1976) and peroxidase (POX) **(**Rescigno *et al*., 1997). It was processed for localization of in-gel α-amylase activity (α-Amy) by Rammesmayer and Praznik method (1992) through gel incubation with a soluble starch containing solution and then stained with iodine solution. Furthermore, native gel was incubated in a mixture of β-naphthyl acetate (5.58 × 10-3 mM, pH 7.5) as a substrate along with the dye coupler Fast Blue RR according to Baker and Manwell (1977) and recently modified by Ahmad *et al.* (2012) to evaluate the localized in-gel β-esterase activity (EST).

The polyacrylamide gel was photographed by a gel documentation system and analyzed by Quantity One software (Version 4.6.2). The band intensity (Int.), band percentage (B%) and relative mobility (Rf) of the separated bands were determined, and the genetic distance (GD) and similarity index (SI%) were calculated to compare treated rats to normal controls.

3. Results

Markers of Oxidative Stress

Data depicted in Table 1 showed a significant decrease in TAC associated with increasing concentrations of LPO and TPC in brain tissues of group 3 rats compared to those of groups (1 & 2) ($p \leq 0.05$). While, no differences were observed in parameters of the antioxidant system in brain of diabetic rats (group 4) and those treated with native *B. variegata* extract (group 5). Treatment of diabetic rats with gold *B. variegata* nano-extract (group 6) caused significant alterations in the antioxidant state, as indicated by decreasing TAC levels with increasing concentrations of LPO and TPC compared to those in control rats and treated groups ($p \leq 0.05$).

Table 1: Oxidative stress marker levels in brain tissues of different groups.

	C gp	Extract gp	Nano-extract gp	Diabetic gp	Diabetic gps treated with Extract	Diabetic gps treated with Nano-extract
TAC (µmol/g)	35.66 ± 0.18	35.52 ± 0.20	12.54 ± 0.14^{ab}	35.00 ± 0.18	34.78 ± 0.32	15.73 ± 0.28^{abc}
LPO (nmol/g)	108.77± 0.62	109.28± 0.61	309.43± 0.82^{ab}	106.79± 0.39	106.98± 0.32	246.78± 2.70^{abc}
TPC (nmol/ mg Protein)	18.15± 0.10	18.06± 0.12	51.63± 0.60^{ab}	18.33± 0.03	17.85± 0.15	41.19± 0.72^{abc}

Data were expressed as mean±SE of five replicates, (a) As compared to control group; (b): As compared to native *B. variegata* extract treated group; (c) As compared to diabetic group.

Markers of the Inflammatory Response

As shown in Table 2, compared with normal control rats (Group 1) and native *B. variegata* extract treated group (Group 2), the ACHE and Aβ levels in brain tissues of group 3 rats were significantly increased ($p \leq 0.05$). On the other hand, in brain tissues of group 4 and group 5 no significant changes were noticed. Treatment of diabetic rats with gold nano-extract (Group 6) caused significant elevation ($p \leq 0.05$) in levels of the aforementioned parameters compared to controls and treated groups.

Rats received gold *B. variegata* nano-extract alone (group 3) showed significant elevation in IL-1β and TNF-α levels compared to groups 1 and 2 (Table 3). Levels of these markers still unchanged in brain of diabetic rats and those treated with native extract. Treatment of diabetic rats with gold *B. variegata* nano-extract caused significant increase ($p \leq 0.05$) in these parameters compared to normal controls and treated rats.

Table 2: Acetylcholine esterase (ACHE) and β-amyloid (Aβ) content in brain tissues of different groups.

	C gp	Extract gp	Nano-extract gp	Diabetic gp	Diabetic gps treated with	
					Extract	Nano-extract
ACHE (ng/g)	1.73 ± 0.02	1.71 ± 0.02	2.58 ± 0.06^{ab}	1.70 ± 0.02	1.69 ± 0.03	2.70 ± 0.02^{abc}
Aβ (pg/g)	7.66 ± 0.12	7.63 ± 0.13	9.24 ± 0.14^{ab}	7.66 ± 0.11	7.65 ± 0.11	8.73 ± 0.09^{abc}

Data were expressed as mean ± SE of five replicates, (a) As compared to control group; (b): As compared to native *B. variegata* extract treated group; (c) As compared to diabetic group.

Table 3: Interleukin-1β and tumor necrosis factor-α levels in brain tissues of different groups.

	C gp	Extract gp	Nano-extract gp	Diabetic gp	Diabetic gps treated with	
					Extract	Nano-extract
IL-1β (pg/g)	380.00 ± 3.58	377.40 ± 4.57	574.00 ± 4.45^{ab}	379.20 ± 4.22	377.60 ± 4.96	478.40 ± 4.02^{abc}
TNF-α (pg/g)	137.20 ± 2.84	138.00 ± 2.79	237.40 ± 2.84^{ab}	138.40 ± 3.14	137.80 ± 2.75	221.60 ± 2.98^{abc}

Data were expressed as mean ± SE of five replicates, (a) As compared to control group; (b): As compared to native *B. variegata* extract treated group; (c) As compared to diabetic group.

Electrophoretic Protein Patterns

Native Protein Pattern

In brains of control rats, the native electrophoretic protein pattern was represented by 6 bands, identified at Rfs 0.08, 0.20, 0.58, 0.67, 0.82, and 0.92 (Int. 112.79, 120.96, 225.84, 135.73, 150.06, and 140.53; B% 16.25, 14.68, 4.28, 16.47, 22.20, and 26.11, respectively) (Fig. 1). The bands at Rfs of 0.08, 0.58, 0.82 and 0.92 were considered common bands. Administration of extract alone caused no physiological difference from controls. In group 3, physiological changes occurred represented by one normal band hiding and 2 abnormal bands identified at Rfs of 0.33 and 0.63 (Int. 127.11 and 136.54; B% 14.81 and 14.01, respectively). The second abnormal band (at Rf = 0.63) is considered the characteristic band. The SI value decreased (SI=76.92%) and GD value increased (GD=23.08%) in gold *B. variegata* nano-extract treated group.

In brain of diabetic rats, the abnormalities in the native protein pattern were represented by one normal band hiding accompanied by the appearance of 3 abnormal bands identified at Rfs 0.33, 0.46, and 0.73 (Int. 128.97, 119.45, and 111.13; B% 15.87, 11.22, and 7.92, respectively). The third abnormal band (at Rf=0.73) is considered the characteristic band. The lowest SI value (SI=71.43%) and the highest GD value (GD=28.57%) were observed in that group.

Treatment of diabetic rats with native *B. variegata* extract restored the native protein pattern physiological state by disrupting the abnormal band and restoring the normal band. Therefore, values of SI increased and the GD values decreased (SI=100.00%; GD=0.00%). Treatment of diabetic rats with gold *B. variegata* nano-extract increased the adverse effect of hiding one band, with 2 abnormal bands identified at Rfs of 0.35 and 0.46 (Int. 131.92 and 121.12; B% 17.87 and 11.33, respectively). No characteristic band was detected in that group. The severity of physiological alterations in the diabetic group was identical to that in the group treated with nano-extract alone. Therefore, the SI and GD values (SI=76.92%; GD=23.08%) were the same in those groups.

Lipid Moiety of Native Protein Pattern

In the brains of controls (Fig. 2), the lipid moiety of native protein pattern was electrophoretically represented by 6 bands identified at Rfs 0.40, 0.45, 0.60, 0.74, and 0.90 (Int. 176.80, 152.87, 148.26, 145.21, and 155.22; B% 27.60, 14.80, 21.29, 14.51, and 21.81, respectively). The bands identified at Rfs 0.40, 0.60, and 0.90 were considered common bands. No characteristic bands were observed in any of the groups. Administration of the native extract alone caused no physiological difference from control group. Treatment with gold *B. variegata* nano-extract alone caused physiological changes, as expressed by the hidden of one normal band and the appearance of an abnormal one at an Rfs of 0.82

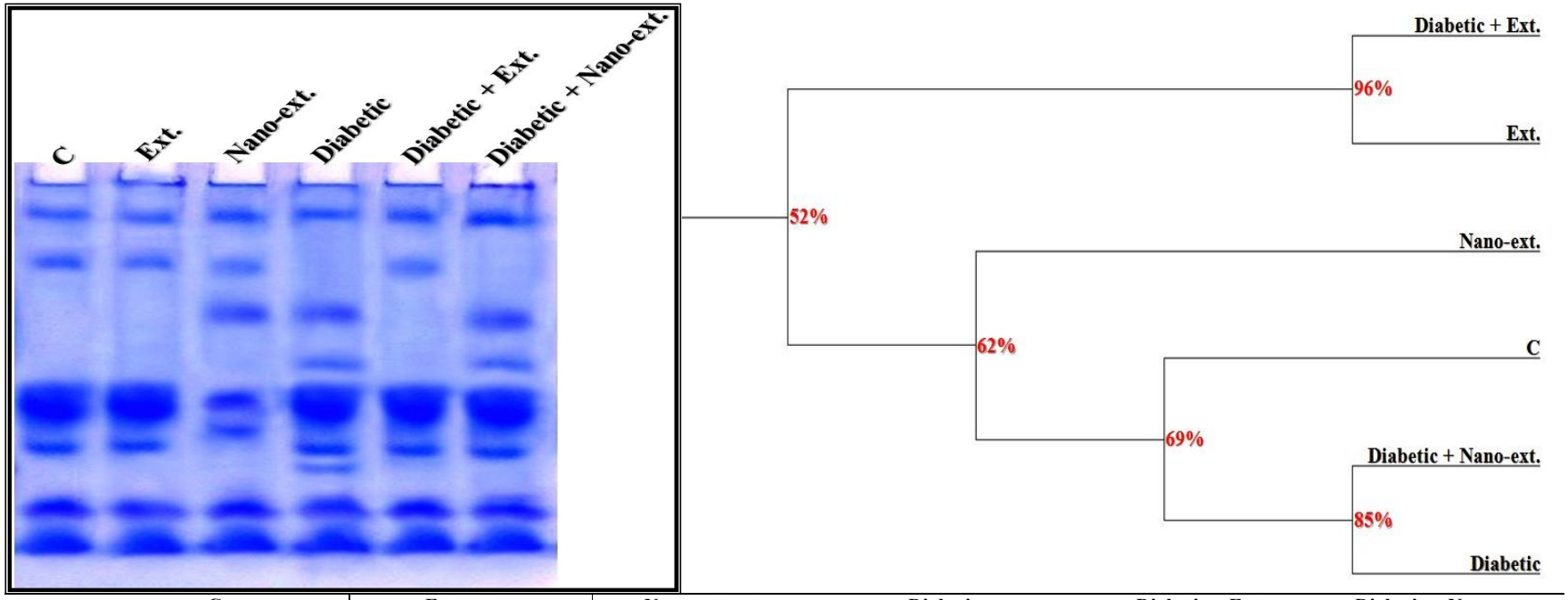

	C gp			Extract gp			Nano-extract gp			Diabetic gp			Diabetic + Ext.			Diabetic + Nano-ext.		
	Rf.	Int.	B%	Rf.	Int.	B%	Rf.	Int.	B%	Rf.	Int.	B%	Rf.	Int.	B%	Rf.	Int.	B%
	0.08	112.79	16.25	0.09	113.80	9.91	0.08	124.88	13.85	0.08	126.57	12.71	0.08	126.66	13.12	0.09	134.10	15.14
	0.20	120.96	14.68	0.20	110.40	12.60	0.21	112.22	11.20	-	-	-	0.21	107.13	12.52	-	-	-
	-	-	-	-	-	-	0.33	127.11	14.81	0.33	128.97	15.87	-	-	-	0.35	131.92	17.87
	-	-	-	-	-	-	-	-	-	0.46	119.45	11.22	-	-	-	0.46	121.12	11.33
	0.58	225.84	4.28	0.57	187.52	30.98	0.55	156.27	14.74	0.56	221.67	4.31	0.57	183.79	29.30	0.58	223.30	4.32
	-	-	-	-	-	-	0.63	136.54	14.01	-	-	-	-	-	-	-	-	-
	0.67	135.73	16.47	0.67	137.37	11.55	-	-	-	0.68	167.54	10.31	0.68	130.86	13.21	0.68	152.00	12.75
	-	-	-	-	-	-	-	-	-	0.73	111.13	7.92	-	-	-	-	-	-
	0.82	150.06	22.20	0.83	136.05	14.71	0.83	178.94	12.90	0.82	153.87	14.95	0.83	153.73	14.29	0.83	156.94	16.71
	0.92	140.53	26.11	0.92	140.43	20.25	0.91	136.03	18.49	0.91	140.29	22.72	0.91	134.87	17.56	0.91	135.65	21.88
SI%		-			100.00			76.92			71.43			100.00			76.92	
GD%		-			0.00			23.08			28.57			0.00			23.08	

Fig. 1: Native electrophoretic protein pattern showing the physiological effect of *B. variegata* extract before and after the incorporation of gold nanoparticles (Au-NPs) against STZ-induced diabetes on the number and arrangement of enzyme bands in brain tissue of rats. Rf.: Relative Mobility, Int.: Band Intensity, B%: Band Percent, SI%: Similarity Percent, GD%: Genetic Distance Percent.

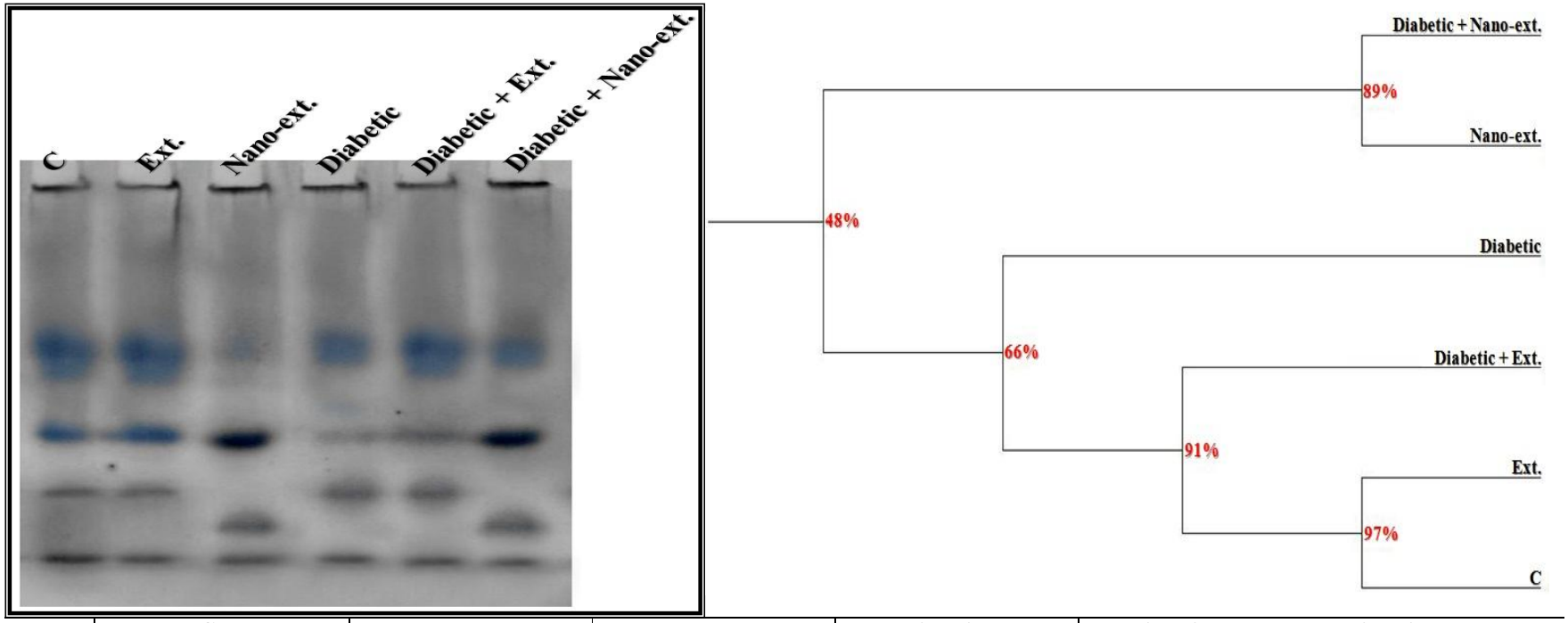

	C gp			Extract gp			Nano-extract gp			Diabetic gp			Diabetic + Ext.			Diabetic + Nano-ext.		
	Rf.	**Int.**	**B%**	**Rf.**	**Int.**	**B%**	**Rf.**	**Int.**	**B%**	**Rf.**	**Int.**	**B%**	**Rf.**	**Int.**	**B%**	**Rf.**	**Int.**	**B%**
	0.40	176.80	27.60	0.41	178.30	26.51	0.40	150.98	13.02	0.40	175.67	6.74	0.39	178.69	26.28	0.40	175.79	5.17
	0.45	152.87	14.80	0.47	145.50	17.95	0.48	122.00	3.37	-	-	-	0.45	155.88	12.90	-	-	-
	0.60	148.26	21.29	0.60	157.74	20.96	0.62	155.64	38.65	0.61	123.75	23.75	0.61	140.98	20.30	0.61	176.61	39.32
	0.74	145.21	14.51	0.74	134.65	14.91	-	-	-	0.74	135.33	37.85	0.75	135.98	24.17	-	-	-
	-	-	-	-	-	-	0.82	137.40	24.64	-	-	-	-	-	-	0.82	135.66	31.35
	0.90	155.22	21.81	0.90	135.14	19.67	0.91	140.28	20.32	0.90	131.21	31.66	0.91	136.83	16.35	0.91	130.71	24.16
SI%		-			100.00			80.00			88.89			100.00			66.67	
GD%		-			0.00			20.00			11.11			0.00			33.33	

Fig. 2: Electrophoretic lipid moiety of native protein pattern showing the physiological effect of *B. variegata* extract before and after the incorporation of gold nanoparticles (Au-NPs) against STZ-induced diabetes on the number and arrangement of the enzyme bands in the brain tissue of rats. Rf.: Relative Mobility, Int.: Band Intensity, B%: Band Percent, SI%: Similarity Percent, GD%: Genetic Distance Percent.

(Int. 137.40; B% 24.64). The SI decreased (SI=80.00%) with increasing GD (GD=20.00%) in the gold *B. variegata* nano-extract treated group.

In the brain of diabetic rats, electrophoretic abnormalities in the lipid moiety of the native protein pattern were shown by the disappearance of a normal band without any abnormal ones. According to the SI and GD values (SI=88.89%; GD=11.11%) in the diabetic group, it was noticed that the severity of physiological alterations induced by gold *B. variegata* nano-extract administration was greater than that in the diabetic group.

Treatment of diabetic rats in group 5 restored the absence of the normal band and thus reestablished the physiological state of the native lipid moiety of native protein pattern. Therefore, physiologically group 5 was similar to the control group (SI=100.00%; GD=0.00%). Treatment of diabetic rats in group 6 increased the adverse effect by hiding one normal band with the appearance of an abnormal one identified at Rf = 0.82 (Int. 135.66; B% 31.35). The severity of physiological disturbances induced by treatment of diabetic group with gold nano-extract was greater than that in the diabetic group and gold nano-extract treated group. Therefore, the lowest SI value (SI=66.67%) and the highest GD value (GD=33.33%) were noticed in that group.

Electrophoretic Isoenzyme Patterns

Catalase Pattern

The electrophoretic CAT isoenzymes in the brains of control rats (Fig. 3) were represented by 3 types identified at Rfs of 0.26, 0.61, and 0.90 (Int. 119.17, 124.54, and 107.64; B% 29.19, 40.04, and 30.76, respectively). All CAT types are considered common bands. No characteristic bands were noticed in treated groups. Administration of *B. variegata* extract and gold nano-extract alone caused no physiological differences from the control group. Therefore, in these groups the highest value of SI (SI=100.00%) and the lowest value of GD (GD=0.00%) were noticed.

In the brains of diabetic rats, physiological changes occurred in CAT pattern, represented by the presence of one abnormal band identified at Rf 0.39 (Int. 118.14; B% 15.90). So, a decrease in the SI value (SI=85.71%) with an increase in the GD value (GD=14.29%) happened.

In diabetic rats treated with native *B. variegata* extract, the integrity of the CAT pattern was restored by hiding the abnormal band. Therefore, the SI values increased and the GD values decreased (SI=100.00%; GD=0.00%). Treatment of diabetic rats with gold nano-extract did not restore the CAT pattern to its normal physiological state and the abnormal band identified at Rf 0.38 (Int. 111.33; B% 16.65). The severity of physiological alterations was identical in the diabetic group and that group treated with nano-extract. Therefore, SI and GD values (SI=85.71%; GD=14.29%) were noticed the same in those groups.

Peroxidase Pattern

The electrophoretic POX pattern in brain of normal controls (Fig. 4) was represented by 6 types at Rfs 0.12, 0.27, 0.41, 0.53, 0.72, and 0.88 (Int. 163.70, 166.40, 115.12, 145.55, 104.12, and 154.14; B% 18.26, 22.55, 6.176, 21.99, 9.26, and 21.76, respectively). The four POX types (POX 2, POX 4, POX 5 and POX 6) identified at Rfs 0.27, 0.53, 0.72 and 0.88 were considered common bands. No characteristic bands were observed in treated groups. The groups treated with native *B. variegata* extract and gold nano-extract alone were physiological similar to control group. Thus, the highest SI value and the lowest GD value (100.00% and 0.00%, respectively) were noticed in those groups.

In brain of diabetic rats, there were physiological changes occurred in POX pattern represented by hiding 2 POX types (POX 1 and POX 3) with presence of abnormal band identified at Rf 0.06 (Int. 154.70; B% 14.30). Therefore, the SI value was decreased (72.73%) and the GD value was increased (27.27%) in that group.

Treatment of diabetic rats with native *B. variegata* extract in group 5 restored the integrity of the POX pattern by restoring the absent types. Thus, physiologically group 5 was similar to control group (SI=100.00% & GD=0.00%). Treatment of diabetic rats with gold nano-extract could not restore integrity of POX pattern to its normal state and the abnormal band still identified at Rf 0.06 (Int. 125.73; B% 27.87). In the diabetic group, severity of the physiological changes was identical to that in the diabetic group treated with nano-extract. Therefore, SI and GD values were noticed equal in those groups (SI=72.73%; GD=27.27%).

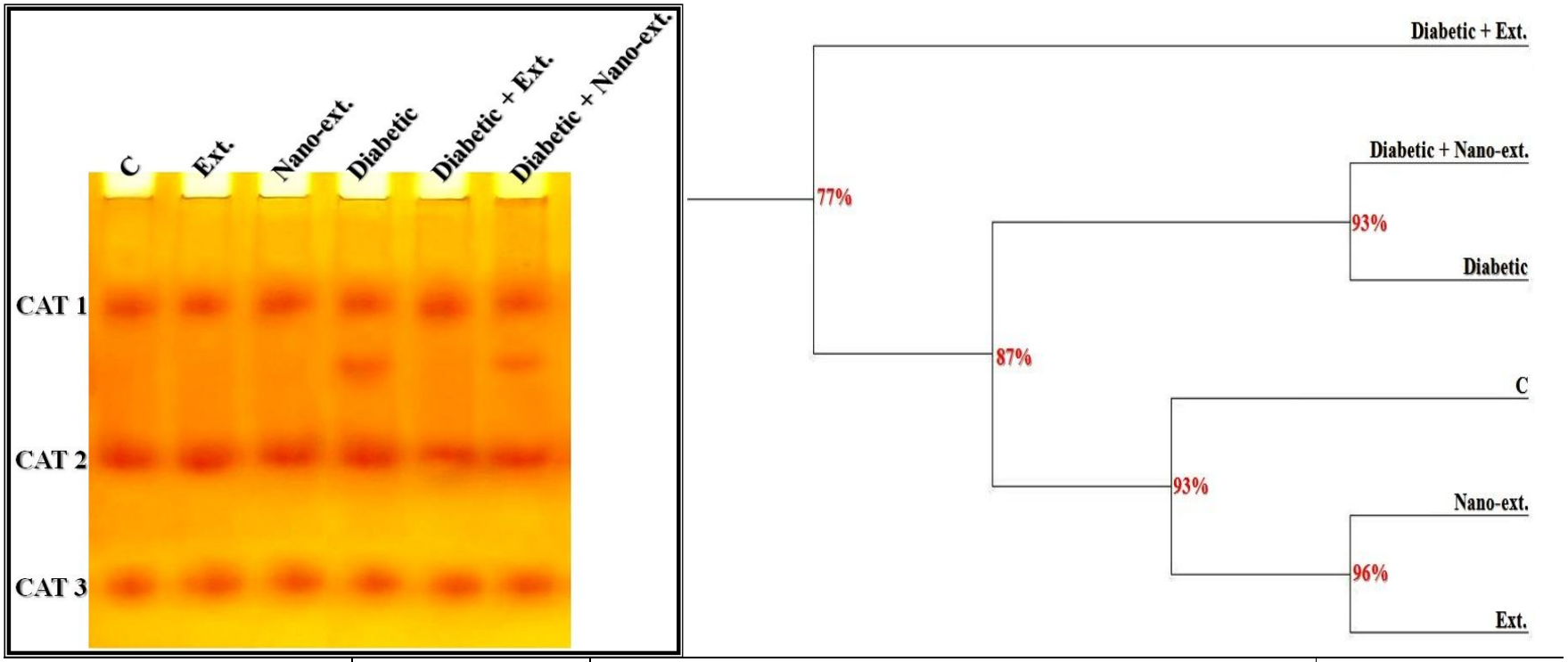

	C gp			Extract gp			Nano-extract gp			Diabetic gp			Diabetic + Ext.			Diabetic + Nano-ext.		
	Rf.	**Int.**	**B%**	**Rf.**	**Int.**	**B%**	**Rf.**	**Int.**	**B%**	**Rf.**	**Int.**	**B%**	**Rf.**	**Int.**	**B%**	**Rf.**	**Int.**	**B%**
CAT 1	0.26	119.17	29.19	0.25	116.57	28.07	0.24	116.31	32.94	0.25	111.83	27.10	0.26	117.63	42.93	0.24	119.94	25.42
	-	-	-	-	-	-	-	-	-	0.39	118.14	15.90	-	-	-	0.38	111.33	16.65
CAT 2	0.61	124.54	40.04	0.61	129.08	36.27	0.60	125.77	35.03	0.60	128.21	31.56	0.59	131.30	27.67	0.61	120.70	31.10
CAT 3	0.90	107.64	30.76	0.90	103.00	35.66	0.89	102.99	32.03	0.89	101.73	25.43	0.90	102.12	29.40	0.90	102.51	26.83
SI%		-			100.00			100.00			85.71			100.00			85.71	
GD%		-			0.00			0.00			14.29			0.00			14.29	

Fig. 3: Native electrophoretic catalase (CAT) isoenzyme pattern showing the physiological effect of *B. variegata* extract before and after the incorporation of gold nanoparticles (Au-NPs) against STZ-induced diabetes on the number and arrangement of the enzyme bands in the brain tissue of rats. Rf.: Relative Mobility, Int.: Band Intensity, B%: Band Percent, SI%: Similarity Percent, GD%: Genetic Distance Percent.

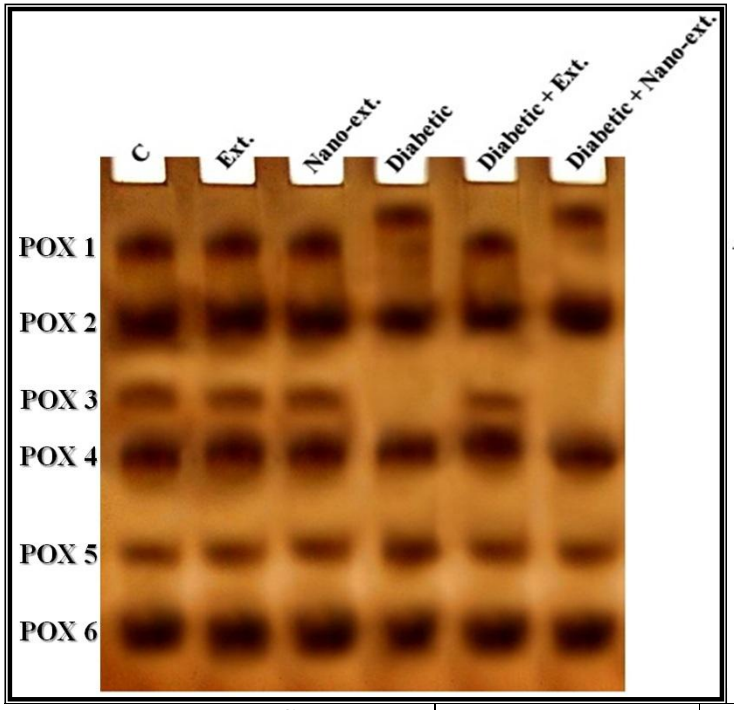

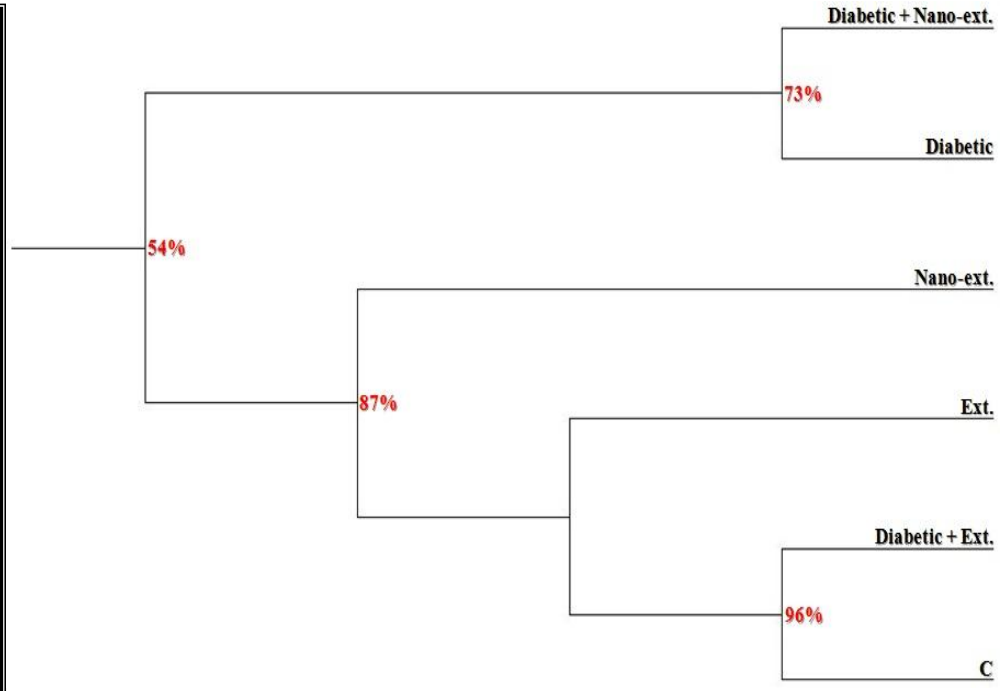

	C gp			Extract gp			Nano-extract gp			Diabetic gp			Diabetic + Ext.			Diabetic + Nano-ext.		
	Rf.	**Int.**	**B%**	**Rf.**	**Int.**	**B%**	**Rf.**	**Int.**	**B%**	**Rf.**	**Int.**	**B%**	**Rf.**	**Int.**	**B%**	**Rf.**	**Int.**	**B%**
	-	-	-	-	-	-	-	-	-	0.06	154.70	14.30	-	-	-	0.06	125.73	27.87
POX 1	0.12	163.70	18.26	0.12	163.44	17.22	0.12	164.83	19.40	-	-	-	0.11	150.63	15.31	-	-	-
POX 2	0.27	166.40	22.55	0.26	157.33	24.76	0.28	128.76	12.96	0.26	154.74	23.14	0.26	157.12	21.37	0.26	241.33	4.60
POX 3	0.41	115.12	6.176	0.41	104.00	4.70	0.42	107.63	9.83	-	-	-	0.43	106.93	8.47	-	-	-
POX 4	0.53	145.55	21.99	0.52	142.92	22.30	0.52	142.98	22.14	0.52	125.34	21.06	0.51	145.49	22.18	0.53	132.33	33.75
POX 5	0.72	104.12	9.26	0.72	107.60	9.72	0.71	109.88	11.57	0.72	125.11	16.40	0.72	119.58	10.72	0.72	108.03	17.77
POX 6	0.88	154.14	21.76	0.88	162.22	21.31	0.89	151.17	24.11	0.88	154.06	25.11	0.88	154.67	21.96	0.90	149.24	16.01
SI%		-			100.00			100.00			72.73			100.00			72.73	
GD%		-			0.00			0.00			27.27			0.00			27.27	

Fig. 4: Native electrophoretic peroxidase (POX) isoenzyme pattern showing the physiological effect of *B. variegata* extract before and after the incorporation of gold nanoparticles (Au-NPs) against STZ-induced diabetes on the number and arrangement of the enzyme bands in the brain tissue of rats. Rf.: Relative Mobility, Int.: Band Intensity, B%: Band Percent, SI%: Similarity Percent, GD%: Genetic Distance Percent.

α-Amylase Pattern

As presented in Fig. 5, in the brains of control rats, the electrophoretic α-Amy pattern was represented by 2 types recognized at Rfs 0.25 and 0.69 (Int. 98.01 and 95.29; B% 42.50 and 57.50, respectively). The α-Amy 2 type (Rf 0.69) is considered a common band. The groups treated with native *B. variegata* extract and gold nano-extract alone were physiological similar to control group. Consequently, highest SI value (SI=100.00%) and the lowest GD value (GD=0.00%) were noticed in those groups.

In the brains of diabetic rats, physiological changes occurred in the α-Amy pattern expressed through hiding the α-Amy 1 type and the presence of one abnormal band (characteristic) identified at Rf 0.11 (Int. 96.88; B% 55.69). Therefore, the SI decreased (SI=50.00%) with increasing GD (GD=50.00%) in that group.

Diabetic rats treated with native *B. variegata* extract and gold nano-extract, the integrity of the α-Amy pattern was restored by hiding the abnormal band and restoring the absent one. Therefore, physiologically these groups are similar to control group (SI=100.00%; GD=0.00%).

Esterase Pattern

Electrophoretic α-EST isoenzymes (Fig. 6) were represented in the brains of control rats by 2 types identified at Rfs 0.14 and 0.63 (Int. 34.28 and 31.67; B% 54.24 and 45.76, respectively). Both types of α-EST are considered common bands. No deviations were observed in group 2 compared to group 1. The physiological changes caused by the gold *B. variegata* nano-extract in group 3 were represented by the existence of abnormal band identified at RF of 0.04 (Int. 60.14; B% 33.68) in the α-EST pattern. Therefore, the SI decreased with increasing GD (SI=80.00%, GD=20.00%) in that group.

Abnormalities in α-EST isoenzyme pattern were represented in brain of diabetic rats by presence of abnormal (characteristic) band at Rf 0.32 (Int. 60.93; B% 40.07). In that group, the SI and GD values were equal to those of gold *B. variegata* nano-extract treated group (SI=80.00% & GD=20.00%).

Treatment of diabetic rats with native *B. variegata* extract (group 5) restored the α-EST isoenzymes pattern physiological state by hiding the abnormal band. Therefore, the SI increased with decreasing GD (SI=100.00% & GD=0.00%). Treatment of diabetic rats with gold *B. variegata* nano-extract increased the deleterious effect by appearance of two abnormal types represented at Rfs 0.04 and 0.52 (Int. 81.72 and 81.83; B% 26.39 and 24.54, respectively). The second abnormal type (Rf 0.52, Int. 81.83 and B% 24.54) is considered as characteristic band. Severity of physiological alterations increased in the diabetic group treated with nano-extract. Therefore, The lowest SI value (SI=66.67%) and the highest GD value (GD=33.33%) were noticed in that group.

As presented in Fig. 7, the electrophoretic β-EST isoenzyme was expressed in the brains of normal rats by 2 types, identified at Rfs 0.38 and 0.68 (Int. 152.35 and 110.52; B% 64.32 and 35.68, respectively). Additionally, the two β-EST types are considered common bands. No characteristic bands were observed in all groups. Lonely, native extract caused no physiological difference from control group. While in the gold *B. variegata* nano-extract treated group, the physiological changes in the β-EST pattern were represented by an abnormal band at Rf of 0.81 (Int. 88.14; B% 16.64). So, the SI value (SI=80.00%) decreased, and the GD value increased (GD=20.00%) in that group.

In the brains of diabetic group, β-EST isoenzyme pattern abnormalities were represented by 2 abnormal bands at Rfs of 0.15 and 0.81 (Int. 166.29 and 73.46; B% 13.76 and 10.22, respectively); thus, the SI value decreased (SI=66.67%) with increasing the GD value (GD=33.33%).

Diabetic rats treated with native *B. variegata* extract in group 5 restored the β-EST isoenzymes pattern physiological state by hiding abnormal bands. Therefore, the SI increased, and the GD values decreased (SI=100.00% and GD=0.00%).

Treatment of diabetic rats in group 6 showed no physiological difference from those in diabetic group. These abnormalities were represented by 2 abnormal types identified at Rfs of 0.13 and 0.82 (Int. 176.13 and 95.37; B% 15.04 and 18.73, respectively). The severity of physiological alterations was identical in the diabetic group and the nano-extract treated group. Therefore, SI & GD values (SI=66.67% and GD=33.33%) were the same in those groups

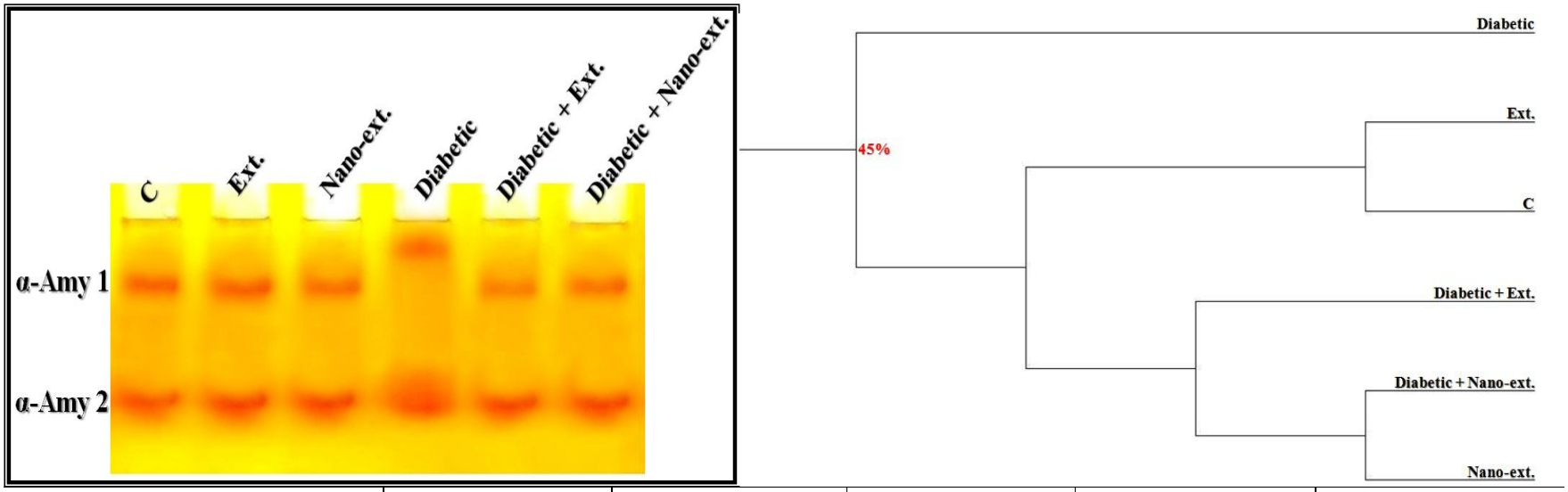

	C gp			Extract gp			Nano-extract gp			Diabetic gp			Diabetic + Ext.			Diabetic + Nano-ext.		
	Rf.	Int.	B%	Rf.	Int.	B%	Rf.	Int.	B%	Rf.	Int.	B%	Rf.	Int.	B%	Rf.	Int.	B%
	-	-	-	-	-	-	-	-	-	0.11	96.88	55.69	-	-	-	-	-	-
α-Amy 1	0.25	98.01	42.50	0.26	98.10	42.40	0.26	96.56	38.41	-	-	-	0.26	91.12	39.63	0.26	96.28	38.06
α-Amy 2	0.69	95.29	57.50	0.70	95.78	57.60	0.70	98.07	61.59	0.71	99.98	44.31	0.70	102.73	60.37	0.70	103.48	61.94
SI%		-			100.00			100.00			50.00			100.00			100.00	
GD%		-			0.00			0.00			50.00			0.00			0.00	

Fig. 5: Native electrophoretic α-amylase (α-Amy) isoenzyme pattern showing the physiological effect of B. variegata extract before and after the incorporation of gold nanoparticles (Au-NPs) against STZ-induced diabetes on the number and arrangement of the enzyme bands in the brain tissue of rats. Rf.: Relative Mobility, Int.: Band Intensity, B%: Band Percent, SI%: Similarity Percent, GD%: Genetic Distance Percent.

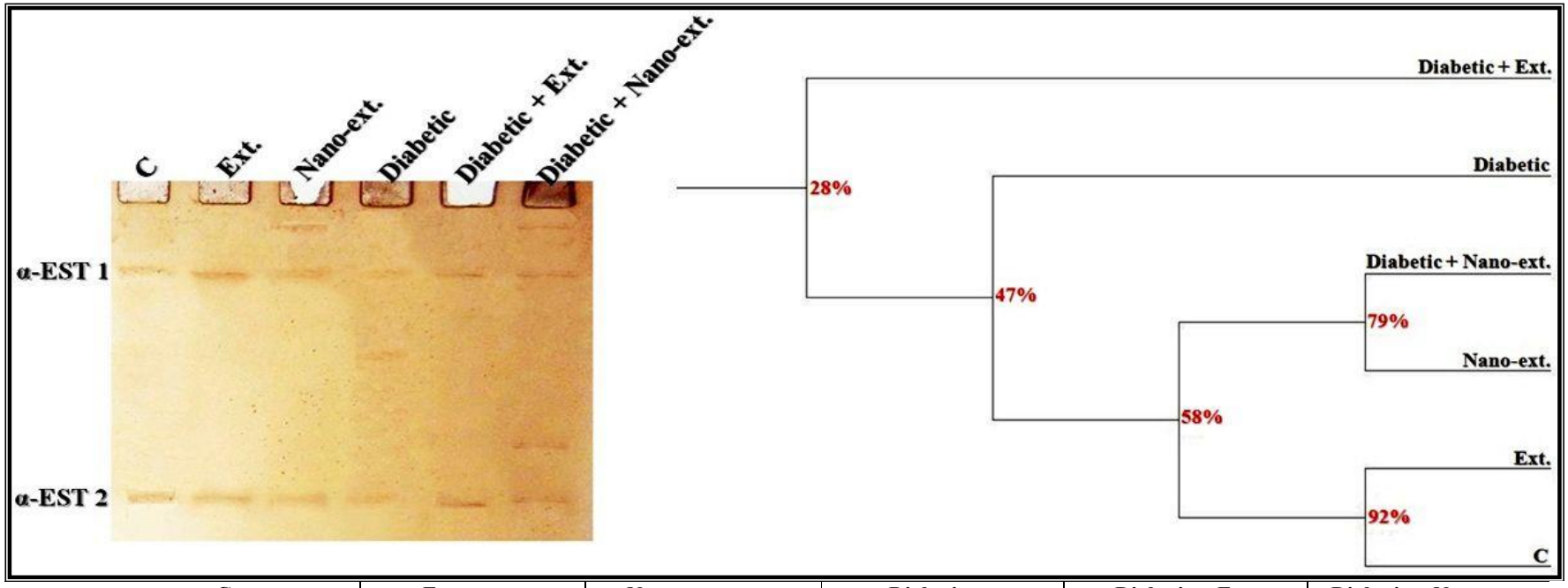

	C gp			Extract gp			Nano-extract gp			Diabetic gp			Diabetic + Ext.			Diabetic + Nano-ext.		
	Rf.	**Int.**	**B%**	**Rf.**	**Int.**	**B%**	**Rf.**	**Int.**	**B%**	**Rf.**	**Int.**	**B%**	**Rf.**	**Int.**	**B%**	**Rf.**	**Int.**	**B%**
	-	-	-	-	-	-	0.04	60.14	33.68	-	-	-	-	-	-	0.04	81.72	26.39
α-EST 1	0.14	34.28	54.24	0.14	49.99	63.9	0.15	53.42	29.92	0.15	60.05	24.13	0.15	78.41	45.22	0.15	81.35	26.27
	-	-	-	-	-	-	-	-	-	0.32	60.93	40.07	-	-	-	0.52	81.83	24.54
α-EST 2	0.63	31.67	45.76	0.63	35.01	36.1	0.63	45.2	36.39	0.63	57.65	35.8	0.64	73.88	54.78	0.63	82.41	22.81
SI%		-			100.00			80.00			80.00			100.00			66.67	
GD%		-			0.00			20.00			20.00			0.00			33.33	

Fig. 6: Native electrophoretic α-esterase (α-EST) isoenzyme pattern showing the physiological effect of *B. variegata* extract before and after the incorporation of gold nanoparticles (Au-NPs) against STZ-induced diabetes on number and arrangement of the enzyme bands in the brain tissue of rats. Rf.: Relative Mobility, Int.: Band Intensity, B%: Band Percent, SI%: Similarity Percent, GD%: Genetic Distance Percent.

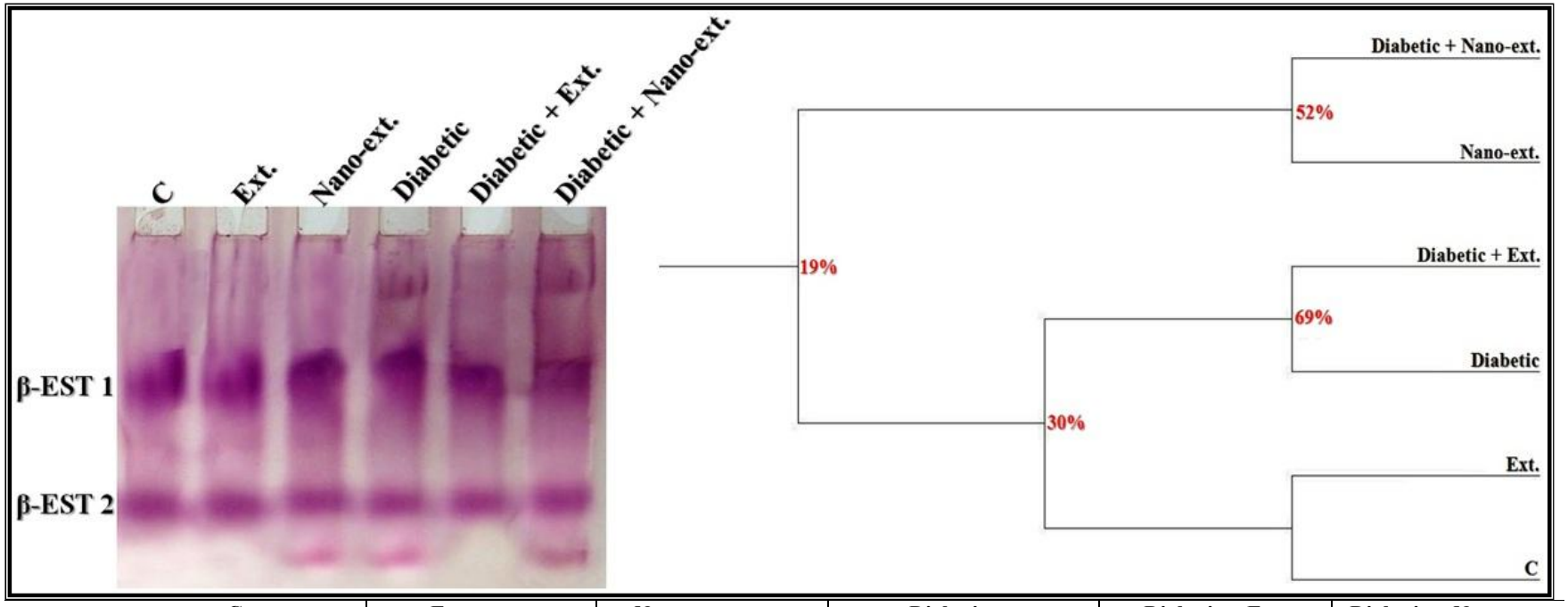

	C gp			Extract gp			Nano-extract gp			Diabetic gp			Diabetic + Ext.			Diabetic + Nano-ext.		
	Rf.	**Int.**	**B%**	**Rf.**	**Int.**	**B%**	**Rf.**	**Int.**	**B%**	**Rf.**	**Int.**	**B%**	**Rf.**	**Int.**	**B%**	**Rf.**	**Int.**	**B%**
	-	-	-	-	-	-	-	-	-	0.15	166.29	13.76	-	-	-	0.13	176.13	15.04
β-EST 1	0.38	152.35	64.32	0.37	160.74	66.69	0.35	205.76	19.42	0.34	169.99	47.95	0.35	196.5	49.97	0.37	183.21	35.2
β-EST 2	0.68	110.52	35.68	0.68	112.63	33.31	0.67	126.26	63.93	0.68	122.31	28.06	0.67	113.28	50.03	0.67	142.46	31.02
	-	-	-	-	-	-	0.81	88.14	16.64	0.81	73.46	10.22	-	-	-	0.82	95.37	18.73
SI%		-			100.00			80.00			66.67			100.00			66.67	
GD%		-			0.00			20.00			33.33			0.00			33.33	

Fig. 7: Native electrophoretic β-esterase (β-EST) isoenzyme pattern showing the physiological effect of *B. variegata* extract before and after the incorporation of gold nanoparticles (Au-NPs) against STZ-induced diabetes on the number and arrangement of the enzyme bands in the brain tissue of rats. Rf.: Relative Mobility, Int.: Band Intensity, B%: Band Percent, SI%: Similarity Percent, GD%: Genetic Distance Percent .

4. Discussion

The toxicity of M-NPs must be carefully examined, even though it has been reported that they are inherently non-toxic. Au-NPs have a size dependent distribution in the body, whereas smaller particles can cross the blood brain barrier (BBB) and can accumulate in all tissues including blood, stomach, liver, kidney, spleen, lung and brain. Smaller sizes cause excessive damage to cells by reactive oxygen species (ROS) production (Arvizo *et al*., 2010; Sani *et al*., 2021). Their toxicity is associated with their reduced stability, releasing of their metal ions into the body and changes in composition due to oxidation of their surface and their tendency to agglomerate. The method of synthesis, size, shape, charge and surface modification by using coating compounds and functionalizing their surface can increase their stability; prevent release of metal ions and the oxidation of their surface which in turn reduce their toxicity (Długosz *et al*., 2020).

It is well known that brain is susceptible to damage by oxidative stress; because of several reasons include unsaturated lipid enrichment, calcium, glutamate, glucose, mitochondria, redox active transition metals, modest antioxidant defense, RNA oxidation and neurotransmitter auto-oxidation. It is susceptible to oxidative stress because it chemically harness diverse reactive species to perform heterogeneous signaling functions (Cobley *et al*., 2018). The integrity and performance of the cells is interrupted by oxygenate radicals (Teleanu *et al*., 2022). Lipid peroxidation is one of the most important causes of oxidative damage that occurs as a result of brain toxicity. Both of the LPO and TPC are the most common markers of oxidative stress and the effect of ROS on lipids and proteins (Muhoberac and Vidal, 2019).

Our study revealed that presence of Au-NPs in the plant extract significantly altered the antioxidant system by decreasing the level of TAC and increasing the concentrations of LPO and TPC in brain tissues ($p \leq 0.05$) compared to control and diabetic groups. Xu *et al.* (2015) reported that M-NPs exhibit a deleterious effect on brain tissue directly through disruption of the blood-brain barrier or via trans-synaptic transport and hence accumulate in brain regions. Dvorakova *et al*. (2022) added that products of peroxidation reaction elevated due to the effect of oxidative stress (a likely mechanism of toxicity of Au-NPs).

The inflammatory mediators were expressed and up-regulated during the nitrosative and oxidative stress and triggered through nuclear factor-κB (NF-κB) activation (Senapati *et al*., 2015; Xu *et al*., 2019). Cholinesterases (ChEs) are enzymes that catalyze the hydrolysis of acetyl choline (which acts as neurotransmitter) into choline and acetic acid. Acetylcholine esterase (AChE) is the most important type of ChEs. It is found in all excitable tissues, whether muscle or nerve peripheral and central cholinergic or adrenergic, sensory or motor, in most erythrocyte and in placental tissues and the neuromuscular junction of skeletal muscle (Khan *et al*., 2023). It plays an effective role in transporting the nerve signals in the nervous system and terminating synaptic transmission through the hydrolysis of the neurotransmitter acetylcholine into acetate and choline (after completing its function) (Rabeler *et al*., 2023).

Administration of gold *B. variegata* nano-extract either alone or in combination with STZ resulted in a significant increase in IL-1β and TNF-α levels in the brain compared to those in the other treated groups. These was in agreement with the results obtained by Ansar *et al.* (2017)**,** who postulated that exposure to nanoparticles orally affected the brain tissues and induced "neurotoxicity" through oxidative and inflammatory mechanisms. Moreover, the proteins that play a role in the inflammatory reactions in brain tissues detected on the surface of the nanoparticles after oral administration (Shim *et al*., 2014; Xu *et al*., 2022). In addition, the levels of ACHE and Aβ in brain tissues were significantly elevated in the nano-extract group and diabetic group treated with nano-extract. This might be due to the direct correlation between ACHE and Aβ content. Therefore, an increase in Aβ, which binds directly to nicotinic receptors, leads to an increase in the ACHE content in and around Aβ plaques **(**Ahmed *et al*., 2011). Furthermore, ACHE can co-localize with Aβ deposits to promote the assembly of Aβ into amyloid fibrils forming Aβ-ACHE complex which is more toxic than amyloid fibrils (Mezeiova *et al*., 2019).

The present results demonstrated that rats received gold *B. variegata* nano-extract alone and diabetic rats treated with nano-extract showed significant ($p \leq 0.05$) increases in IL-1β and TNF-α levels compared to normal controls and diabetic groups. This finding was in agreement with Ansar *et al.* (2017) and was consequently approved by Ling *et al.* (2019), who revealed that "neurotoxicity"

induced *via* inflammatory and oxidative mechanisms as a result of oral administration of M-NPs alone or in combination with plant extracts.

Gold *B. variegata* nano-extract caused physiological changes in the electrophoretic protein pattern through hiding one band and appearance of two abnormal ones when administrated either alone or as a treatment for diabetic rats. Also, Shim *et al.* (2014) emphasized that due to the M-NPs ability to react with proteins in brain tissues, changes in native protein pattern takes place. Moreover, these changes might be because of the reaction of the most abundant brain proteins with a broad range of reactive species (oxidative stress) that cause chemical changes (cross-linking, fragmentation, aggregation and oxidation) in the protein molecules (Hawkins *et al*., 2009; Dąbkowska *et al*., 2021).

Our results revealed that gold *B. variegata* nano-extract caused physiological changes in the electrophoretic lipid moiety of the protein pattern by hiding one normal band and the appearance of an abnormal one in nano-extract group and diabetic group treated with nano-extract. This might be attributed to reactive species products accumulation that occurred as a result of lipid portion attack and a reduction in antioxidant defenses that leads to denaturation and oxidative modifications of the lipid moieties of proteins (El-Sayed *et al*., 2018).

In the brains of diabetic rats, native protein pattern changes were illustrated by appearance of three abnormal bands with hiding normal one, which might indicate a decrease in the antioxidant defenses and glycation (non-enzymatic) of the native proteins via sugar reacting with the protein portions (Blasiak *et al*., 2004; Ullah *et al*., 2019). Furthermore, glycation leads to decreasing the chaperone efficiency which is responsible for the protein folding to exhibit its biological role (Niforou *et al*., 2014).

In the brains of diabetic rats, electrophoretic lipid moiety of native protein pattern abnormalities were verified by disappearance of one band that might be due to disturbances in cholesteryl esterase and cholesterol hydrolysis required in addition to the role of ROS in initiating one-electron reduction or one-electron oxidation reactions in several biological systems and the oxidative theory that classically admits lipoproteins oxidation involvement (Grindel *et al*., 2016). Furthermore, in brain tissues there was natural binding between lipoproteins and proteins. Therefore, changes in the native protein pattern lipid moiety might be related to altering the protein pattern in brain tissue (Bonilha *et al*., 2021).

The antioxidant enzymes activity varies from tissue to tissue and is considered tissue-dependent tools of the antioxidant system. Both of POX and CAT had a potent role in free radicals detoxification (Abbas *et al*., 2018). Changes in the antioxidants activity of diabetic rats may be because of the degeneration of the protein contents and / or due to metabolic pathways alterations as a result of free radicals attack (Ushio-Fukai *et al*., 2021). The present study revealed that the physiological changes that were detected electrophoretically in the brains of diabetic rats represented by existence of one abnormal band in CAT pattern and hiding 2 normal types POX pattern and that was in compliance with Al-Enazi (2014) findings, who stated that variations in the electrophoretic POX and CAT patterns might be attributed to the glycation of enzymes that inhibit their activities. Likewise, in the brains of diabetic rats, the electrophoretic CAT and POX alterations might be due to H_2O_2 accumulation, uncontrolled production of ROS and oxidative stress. This leads consequently to oxidative damage, as demonstrated by perturbations in different antioxidant enzymes (De Freitas *et al*., 2014). Reduction in the activities of these enzymes could be due to direct effects of ROS on the enzymes or the protein portion of these enzymes. Thus, these ROS can change the immunologic and physicochemical properties of endogenic CAT and POX enzymes (Rajput *et al*., 2021).

α-Amylase (a digestive enzyme exists in pancreatic juice and saliva), catalyzes the hydrolysis of the α-(1,4)-D-glycosidic linkages of starch and other glucose polymers for the degradation of dietary carbohydrates to oligosaccharides and disaccharides. It is considered a potential target for diabetes (Patil *et al*., 2022). Throughout our study, physiological alterations in the α-Amy pattern in the brains of diabetic rats were illustrated by existence of one abnormal band with hiding normal α-Amy type. In accordance with Udia *et al.* (2016), who postulated that abnormalities in the α-Amy pattern might be attributed to changes in amylase mRNA levels in parallel to changes in amylase protein levels. Moreover, the α-Amy pattern might change due to hormonal and metabolic alterations sequel to DM (Onikanni *et al*., 2021).

Esterases are large class of enzymes used as prognostic markers for various chronic diseases (Belinskaia *et al*., 2021). These lysosomal lipolytic enzymes stimulate the hydrolysis of neutral lipids

ester bonds (lipid deposits and lipoprotein components) and their cleavage into the corresponding carboxylic acids (Benjamin *et al*., 2015). They have numerous molecular forms distinguished by their molecular weights and hydrodynamic properties, as visualized by substrate staining using α- and β-naphthyl acetate in the presence of a dye coupler (Fast Blue RR salt) (Napon *et al*., 2018). Esterase enzymes in the brain play an important role in communication and neurotransmission, where they are associated with membrane structures and exhibit their activity through breakdown stimulation of acetylcholine released during nervous stimulation (Srividhya *et al*., 2012; Sam and Bordoni, 2023). Therefore, it was chosen to be studied during the current study. Due to the presence of active thiol groups in the EST enzymes, electrophoresis is considered the most suitable technique for identifying the EST pattern (Abdalla *et al*., 2015).

Our study revealed that gold *B. variegata* nano-extract caused physiological alterations represented by the existence of one or more abnormal bands when administrated either alone or as a treatment for diabetic rats. This might refer to the presence of the Au-NPs that are responsible for the mutagenicity detected electrophoretically in the α- and β-EST patterns, which might be attributed to their effect on the membrane-bound enzymes that reflect changes in the physical state of the membrane lipids and are sensitive to alterations in membrane fluidity (Seif *et al*., 2017). Likewise, Aboulthana *et al.* (2016) reported that the integrity of protein molecules was affected by ROS through polypeptide chain fragmentation due to sulfhydryl-mediated cross linking of labile amino acids, and changes in the fractional activity of different isoenzymes are correlated with alterations in the protein expression rate secondary to DNA damage induced by ROS. Therefore, this leads to structural alterations in protein portion of native enzymes. If no alterations occurred in protein expression, there were no changes in the enzymatic activity (Djordjevic *et al*., 2010; Abulyazid *et al*., 2017; El-Sayed *et al*., 2018).

In the brains of diabetic rats, electrophoretic abnormalities in the α- and β-EST isoenzyme patterns were represented by the existence of one or more abnormal bands. This might refer to enhancement of oxidative stress and the production of excessive ROS, which consequently results in altered albumin structure and function (Ehtewish *et al*., 2022). Furthermore, the EST pattern characteristic changes might be attributed to changes in the glycosylation of the EST types, which reflects consequently changes in the glycosylated EST forms. The abnormal occurrence of the glycosylation process affected EST stability and increases the probability of protein degradation (Saxena *et al*., 1997).

Administration of the native *B. variegata* extract ameliorated the physiological abnormalities in all electrophoretic protein (native protein and lipid moieties of the native protein) and isoenzyme (CAT, α-Amy, POX, β-EST and α-EST) patterns induced in the brains of diabetic rats. Therefore, the highest SI value (SI=100.00%) was noticed with all groups treated with native *B. variegata* extract. In agreement with Azevedo *et al.* (2006) and Abdel-Halim *et al.* (2020), *the* ameliorative effect of *B. variegata* extract refers to its anti-diabetic effect, which is related to insulin-like proteins existence. Furthermore, active constituents (phenolic compounds) that possesses high radicals scavenging and antioxidant activities are present. Moreover, the scavenging efficiency of the native extract depends on the phenols concentration and the hydroxyl group numbers and position that stimulate antioxidant enzyme activity to overcome the attack of free radicals targeting these macromolecules (Rao and Mohan, 2017; Hussien *et al*., 2024). In addition, restoring the electrophoretic protein and isoenzymes patterns as a result of administration of the native *B. variegata* extract might refer to the role of polyphenols that revealing the anti-glycating activity through other mechanisms, irrespective of glycation inhibition (Muthenna *et al*., 2012; Yeh *et al*., 2017).

5. Conclusion

Despite the therapeutic efficiency of Au-NPs, they may have toxic effects on human body due to their high ability to pass BBB and accumulate in the brain leading to neurotoxicity. Therefore, it was necessary to investigate their toxicity. The study concluded that the administration of gold *B. variegata* nano-extract during the treatment of diabetic rats caused a significant decrease in TAC associated with increasing concentrations of peroxidation products (LPO and TPC), levels of ACHE and Aβ as well as elevating IL-1β and TNF-α level in brain tissues as inflammatory markers. Furthermore, the native electrophoretic protein and isoenzyme (α-Amy, α-EST and β-EST) patterns showed that the administration of gold *B. variegata* nano-extract caused physiological alterations

represented by hiding one or more of normal bands and the appearance of one or more abnormal bands. Regarding the electrophoretic CAT and POX patterns, the gold nano-extract had no adverse (undesirable) effects. Administration of native *B. variegata* extract exhibited a greater physiological ameliorative effect against the deleterious effects induced in the brains of diabetic rats.

References

Abbas, G., B. Murtaza, I. Bibi, M. Shahid, N.K. Niazi, M.I. Khan, M. Amjad, M. Hussain, Natasha. 2018. Arsenic Uptake, Toxicity, Detoxification, and Speciation in Plants: Physiological, Biochemical, and Molecular Aspects. Int J Environ Res Public Health, 15(1):59.

Abdalla, M.S., H.M. Sharada, I. Abulyazid, et al., 2015. Ameliorative effect of salicin against gamma irradiation induced electrophoretic changes in brain tissue in male rats. UK J Pharm Biosci, 3(2):29-41.

Abdel-Halim, A.H., A.A. Fyiad, W.M. Aboulthana, et al., 2020. Assessment of the Anti-diabetic Effect of *Bauhinia variegata* Gold Nano-Extract against Streptozotocin Induced Diabetes Mellitus in Rats. Journal of Applied Pharmaceutical Science,10(05):077-91.

Aboulthana, W.M., N.E. Ibrahim, N.M. Osman, et al., 2020. Evaluation of the Biological Efficiency of Silver Nanoparticles Biosynthesized Using *Croton tiglium L.* Seeds Extract against Azoxymethane Induced Colon Cancer in Rats. Asian Pacific Journal of Cancer Prevention, 21(5):1369-89.

Aboulthana, W.M., M. Ismael, and H.S. Farghaly, 2016. Assessment of mutagenicity induced by toxic factors affecting ovarian tissue in rats by electrophoresis and molecular dynamic modeling. Int. J. Curr. Pharm. Rev. Res., 7(6):347-59.

Aboulthana, W.M., N.I. Omar, E.A. Hasan, et al., 2022. Assessment of the Biological Activities of Egyptian Purslane (*Portulaca oleracea*) Extract after Incorporating Metal Nanoparticles, *in vitro* and *in vivo* Study. Asian Pacific Journal of Cancer Prevention, 23(1):287-310.

Aboulthana, W.M., W.G. Shousha, E.A. Essawy, et al., 2021. Assessment of the Anti-Cancer Efficiency of Silver *Moringa oleifera* Leaves Nano-extract against Colon Cancer Induced Chemically in Rats. Asian Pacific Journal of Cancer Prevention, 22(10):3267-86.

Abulyazid, I., S.A. Abd Elhalim, H.M. Sharada, et al., 2017. Hepatoprotective Effect of Carob Pods Extract (*Ceratonia siliqua* L.) against Cyclophosphamide Induced Alterations in Rats. International Journal of Current Pharmaceutical Review and Research, 8(2):149-62.

Ahmad, A., V. Maheshwari, A. Ahmad, et al., 2012. Observation of esterase-like-albumin activity during N'-nitrosodimethyl amine induced hepatic fibrosis in a mammalian model. Maced. J. Med. Sci., 5(1):55-61.

Ahmed, H.H., W.G. Shousha, R.M. Hussein, et al., 2011. Potential role of some nutraceuticals in the regression of Alzheimer's disease in an experimental animal model. Turk J Med Sci., 41(3):455-466.

Al-Enazi, M.M., 2014. Combined Therapy of Rutin and Silymarin has More Protective Effects on Streptozotocin-Induced Oxidative Stress in Rats. Journal of Applied Pharmaceutical Science, 4(01):021-8.

Ansar, S., M. Abudawood, S.S. Hamed, et al., 2017. Exposure to zinc oxide nanoparticles induces neurotoxicity and proinflammatory response: amelioration by hesperidin. Biol Trace Elem Res., 175:360-6.

Arvizo R, Bhattacharya R, Mukherjee P. Gold nanoparticles: opportunities and challenges in nanomedicine. Expert Opin Drug Deliv. 2010;7(6):753-63.

Azevedo, C.R., F.M. Maciel, L.B. Silva, et al., 2006. Isolation and intracellular localization of insulin-like proteins from leaves of *Bauhinia variegate*. Braz. J. Med. Biol. Res., 39(11):1435-44.

Baker, C.M.A., and C. Manwell, 1977. Heterozygosity of the sheep: Polymorphism of 'malic enzyme', isocitrate dehydrogenase (NADP+), catalase and esterase. Aust. J. Biol. Sci., 30(1-2):127-40.

Belinskaia, D.A., P.A. Voronina, V.I. Shmurak, R.O. Jenkins, and N.V. Goncharov, 2021. Serum Albumin in Health and Disease: Esterase, Antioxidant, Transporting and Signaling Properties. Int. J. Mol. Sci., 22(19):10318.

Benjamin, S., S. Pradeep, M.K.S. Josh, et al., 2015. A monograph on the remediation of hazardous phthalates. J. Hazard Mater., 298:58-72.

Berbudi, A., N. Rahmadika, A.I. Tjahjadi, and R. Ruslami, 2020. Type 2 Diabetes and its Impact on the Immune System. Curr. Diabetes Rev., 16(5):442-449.

Blasiak, J., M. Arabski, R. Krupa, K. Wozniak, M. Zadrozny, J. Kasznicki, M. Zurawska, and J. Drzewoski, 2004. DNA damage and repair in type 2 diabetes mellitus. Mutat. Res., 554(1-2):297-304.

Bonilha, I., F. Zimetti, I. Zanotti, B. Papotti, and A.C. Sposito, 2021. Dysfunctional High-Density Lipoproteins in Type 2 Diabetes Mellitus: Molecular Mechanisms and Therapeutic Implications. J. Clin. Med., 10(11):2233.

Borai, I.H., A.M. Ibrahim, M.M. Ali, M.M. Abd El-Hamid, and A.G. Hussien, 2016. The Role of Abnormal Ketone Bodies during Insulin Deficiency in Streptozotocin Induced Diabetes. International Journal of Current Pharmaceutical Review and Research. 1;7(2):121-8.

Bradford, M.M., 1976. A rapid and sensitive method for the quantitation of microgram quantities of protein utilizing the principle of protein dye binding. Anal. Biochem., 72:248-54.

Chen, C., C.M. Cohrs, J. Stertmann, et al., 2017. Human beta cell mass and function in diabetes: recent advances in knowledge and technologies to understand disease pathogenesis. Mol. Metab., 6(9):943-57.

Cobley, J.N., M.L. Fiorello, and D.M. Bailey, 2018. 13 reasons why the brain is susceptible to oxidative stress. Redox Biol., 15:490-503.

Dąbkowska, M., Z. Ulańczyk, K. Łuczkowska, D. Rogińska, A. Sobuś, M. Wasilewska, M. Olszewska, K. Jakubowska, and B. Machaliński, 2021. The role of the electrokinetic charge of neurotrophis-based nanocarriers: protein distribution, toxicity, and oxidative stress in in vitro setting. J Nanobiotechnology, 19(1):258.

Darwesh, O.M., H. Moawad, O.S. Barakat, et al., 2015. Bioremediation of textile reactive blue azo dye residues using nanobiotechnology approaches. Research Journal of Pharmaceutical Biological and Chemical Sciences, 6:1202-11.

De Freitas, R.B., P.R. Augusti, E.R. De Andrade, et al., 2014. Black Grape Juice Protects Spleen from Lipid Oxidation Induced by Gamma Radiation in Rats. Food Biochem., 38:119-27.

Djordjevic, J., A. Djordjevic, M. Adzic, A. Niciforovic, and M.B. Radojcic, 2010. Chronic stress differentially affects antioxidant enzymes and modifies the acute stress response in liver of Wistar rats. Physiol Res., 59(5):729-736.

Długosz, O., K. Szostak, A. Staroń, et al., 2020. Methods for Reducing the Toxicity of Metal and Metal Oxide NPs as Biomedicine. Materials (Basel)., 13(2):279.

Dvorakova, M., L. Kuracka, I. Zitnanova, S. Scsukova, J. Kollar, K. Konarikova, and L. Laubertova, 2022. Assessment of the Potential Health Risk of Gold Nanoparticles Used in Nanomedicine. Oxid. Med. Cell Longev., 4685642.

Ehtewish, H., A. Arredouani, and O. El-Agnaf, 2022. Diagnostic, Prognostic, and Mechanistic Biomarkers of Diabetes Mellitus-Associated Cognitive Decline. Int. J. Mol. Sci., 23(11):6144.

Elia, P., R. Zach, S. Hazan, et al., 2014. Green synthesis of gold nanoparticles using plant extracts as reducing agents. Int. J. Nanomedicine, 9:4007-21.

EL-Mohandes, N., G. Yee, B.S. Bhutta, et al., 2023. Pediatric Diabetic Ketoacidosis.. In: StatPearls [Internet]. Treasure Island (FL): StatPearls Publishing.

El-Sayed, A.E.B., W.M. Aboulthana, A.M. El-Feky, N.E. Ibrahim, and MM. Seif, 2018. Bio and phyto-chemical effect of Amphora coffeaeformis extract against hepatic injury induced by paracetamol in rats. Mol Biol Rep., 45(6):2007-2023.

Engelmann, H., D. Novick, and D. Wallach, 1990. Two tumor necrosis factor-binding proteins purified from human urine. Evidence for immunological cross-reactivity with cell surface tumor necrosis factor receptors. J Biol Chem., 265:1531-63.

Grindel, A., B. Guggenberger, L. Eichberger, C. Pöppelmeyer, M. Gschaider, A. Tosevska, G. Mare, D. Briskey, H. Brath, and K.H. Wagner, 2016. Oxidative Stress, DNA Damage and DNA Repair in Female Patients with Diabetes Mellitus Type 2. PLoS One., 11(9):e0162082.

Hago, S., E.A. Mahrous, M. Moawad, S. Abdel-Wahab, E. Abdel-Sattar, 2021. Evaluation of antidiabetic activity of Morusnigra L. and Bauhinia variegata L. leaves as Egyptian remedies used for the treatment of diabetes. Nat. Prod. Res., 35(5):829-835.

Hames, B.D., 1990. One dimensional polyacrylamide gel electrophoresis. In: Hames BD and Rickwood D (eds) Gel Electrophoresis of Proteins. 2nd Edition, Oxford University Press New York, 382.

Hawkins. C.L., P.E. Morgan, and M.J. Davies, 2009. Quantification of protein modification by oxidants. Free Radic Biol. Med., 46(8):965-88.

Hussien, A.G., A.A. Fyiad, M.M. Ali, and A.E. Mahmoud, 2024. The Influence of Syzygium aromaticum Ethanolic Extract Against Streptozotocin-Induced Diabetic Rats. Egyptian Journal of Chemistry, 67(2):357-369.

Kamal, Y., T. Khan, I. Haq, S.S. Zahra, M.H. Asim, I Shahzadi, A Mannan, and N. Fatima, 2022. Phytochemical and biological attributes of *Bauhinia variegata* L. (Caesalpiniaceae). Braz J. Biol., 82:e257990.

Khan, S.A., M.J. Akhtar, U. Gogoi, D.U. Meenakshi, and A. Das, 2023. An Overview of 1,2,3-triazole-Containing Hybrids and Their Potential Anticholinesterase Activities. Pharmaceuticals (Basel)., 16(2):179.

Khandanlou, R., V. Murthy, and H. Wang, 2020. Gold nanoparticle-assisted enhancement in bioactive properties of Australian native plant extracts, *Tasmannia lanceolata* and *Backhousia citriodora*. Materials Science and Engineering, C., 112:110922.

Koracevic, D., G. Koracevic, V. Djordjevic, et al., 2001. Method for the measurement of antioxidant activity in human fluids. Journal of Clinical Pathology, 54(5):356-61.

Kulkarni, Y.A., and M.S. Garud, 2016. *Bauhinia variegata* (Caesalpiniaceae) leaf extract: An effective treatment option in type I and type II diabetes. Biomed & Pharmacoth., 83:122-9.

Levine, R.L., J.A. Williams, E.R. Stadtman, et al., 1994. Carbonyl assays for determination of oxidatively modified proteins. Methods Enzymol., 233:346-57.

Ling, L., Y. Jiang, Y. Liu, H. Li, A. Bari, R. Ullah, J. Xue, 2019. Role of gold nanoparticle from Cinnamomum verum against 1-methyl-4-phenyl-1, 2, 3, 6-tetrahydropyridine (MPTP) induced mice model. J. Photochem. Photobiol. B., 201:111657.

Liu, P., X. Yang, J. Niu, and C. Hei, 2022. Hyperglycemia aggravates ischemic brain damage *via* ERK1/2 activated cell autophagy and mitochondrial fission. Front Endocrinol (Lausanne)., 13:928591.

Mahomoodally, M.F., D. Lobine, M.C.N. Picot-Allain, N. Sadeer, S. Jugreet, and G. Zengin, 2021. Conventional and Non-Conventional Targets of Natural Products in the Management of Diabetes Mellitus and Associated Complications. Curr. Med. Chem., 28(23):4638-4669.

Mamillapalli, V., A.M. Atmakuri, and P. Khantamneni, 2016. Nanoparticles for Herbal Extracts. Asian Journal of Pharmaceutics, 10(2): S54-60.

March, C.J., B. Mosley, A. Larsen, et al., 1985. Cloning, sequence and expression of two distinct human interleukin-1 complementary DNAs. Nature, 315:641-7.

Mezeiova, E., K. Chalupova, E. Nepovimova, L. Gorecki, L. Prchal, D. Malinak, K. Kuca, O. Soukup, and J. Korabecny, 2019. Donepezil Derivatives Targeting Amyloid-β Cascade in Alzheimer's Disease. Curr Alzheimer Res., 16(9):772-800.

Muhoberac, B.B., and R. Vidal, 2019. Iron, Ferritin, Hereditary Ferritinopathy, and Neurodegeneration. Front Neurosci., 13:1195.

Muthenna, P., C. Akileshwari, and G.B. Reddy, 2012. Ellagic acid, a new antiglycating agent: its inhibition of *N*ϵ-(carboxymethyl) lysine. Biochem. J., 442(1):221-2.

Napon, G., A.J. Dafferner, A. Saxena, and O. Lockridge, 2018. Identification of Carboxylesterase, Butyrylcholinesterase, Acetylcholinesterase, Paraoxonase, and Albumin Pseudoesterase in Guinea Pig Plasma through Nondenaturing Gel Electrophoresis. Comp. Med., 68(5):367-374.

Niforou, K., C. Cheimonidou, and I.P. Trougakos, 2014. Molecular chaperones and proteostasis regulation during redox imbalance. Redox Biol., 2:323-32.

Ohkawa, H., N. Ohishi, and K. Yagi, 1979. Assay for lipid peroxides in animal tissues by thiobarbituric acid reaction. Anal Biochem., 95:351-8.

Onikanni, A.S., B. Lawal, A.O. Olusola, J.O. Olugbodi, S. Sani, B.O. Ajiboye, O.B. Ilesanmi, M. Alqarni, G. Mostafa-Hedeab, A.J. Obaidullah, G.E. Batiha, and A.T.H. Wu, 2021. *Sterculia tragacantha* Lindl Leaf Extract Ameliorates STZ-Induced Diabetes, Oxidative Stress, Inflammation and Neuronal Impairment. J. Inflamm. Res., 14:6749-6764.

Patil, S.M., R.M. Martiz, A.M. Satish, A.M. Shbeer, M. Ageel, M. Al-Ghorbani, and L. Ranganatha, 2022. 5th, Parameswaran S, Ramu R. Discovery of Novel Coumarin Derivatives as Potential Dual Inhibitors against α-Glucosidase and α-Amylase for the Management of Post-Prandial Hyperglycemia via Molecular Modelling Approaches. Molecules, 27(12):3888.

Rabeler, C., T. Gong, D. Ireland, O. Cochet-Escartin, and E.S. Collins, 2023. Acetylcholinesterase Activity Staining in Freshwater Planarians. Curr. Protoc., 3(2):e674.

Rajput, V.D., Harish, R.K. Singh, K.K. Verma, L. Sharma, F.R. Quiroz-Figueroa, M. Meena, V.S. Gour, T. Minkina, S. Sushkova, and S. Mandzhieva, 2021. Recent Developments in Enzymatic Antioxidant Defence Mechanism in Plants with Special Reference to Abiotic Stress. Biology (Basel)., 10(4):267.

Rammesmayer, G., and W. Praznik, 1992. Fast and sensitive simultaneous staining method of Q-enzyme, α-amylase, R-enzyme, phosphorylase and soluble starch synthase separated by starch: polyacrylamide gel electrophoresis. J. Chromatogr., 623(2):399-402.

Rao, P.S., and G.K. Mohan, 2017. *In vitro* alpha-amylase inhibition and *in vivo* antioxidant potential of *Momordica dioica* seeds in streptozotocin-inducedoxidative stress in diabetic rats. Saudi J Biol Sci., 24(6):1262–1267.

Rashid, K.I., 2014. Detection of Insulin-Like Protein and Some Active Compounds in *Bauhinia Variegata* Linn. Leaf Ethanolic Extracts and the Effect in Reducing Blood Glucose Levels in Mice. Journal of Biotechnology Research Center,8(2):76-83.

Rescigno, A., E. Sanjust, L. Montanari, et al., 1997. Detection of laccase, peroxidase, and polyphenol oxidase on a single polyacrylamide gel electrophoresis. Anal Lett., 30:2211-20.

Sachdewa, A., R. Nigam, and L.D. Khemani, 2001. Hypoglycemic effect of *Hibiscus rosasinensis L.* leaf extract in glucose and streptozotocin induced hyperglycemic rats. Indian J Exp Biol., 39(3):284-6.

Sam, C., and B. Bordoni, 2023.Physiology, Acetylcholine. In: StatPearls [Internet]. Treasure Island (FL): StatPearls Publishing.

Sani, A., C. Cao, and D. Cui, 2021. Toxicity of gold nanoparticles (AuNPs): A review. Biochem.Biophys. Rep., 26:100991.

Saxena, A., L. Raveh, Y. Ashani, and B.P. Doctor, 1997. Structure of glycan moieties responsible for the extended circulatory life time of fetal bovine serum acetylcholinesterase and equine serum butyrylcholinesterase. Biochemistry, 36(24):7481-9.

Seif, M.M., O.A. Ahmed-Farid, and W.M. Aboulthana, 2017. Evaluation of the Protective Effect of *Acacia senegal* Extract against di-(2-ethylhexyl phthalate) Induced Hepato- and Neurotoxicity in Rats. Annual Research & Review in Biology, 19:1-17.

Senapati, V.A., A. Kumar, G.S. Gupta, et al., 2015. ZnO nanoparticles induced inflammatory .response and genotoxicity in human blood cells: A mechanistic approach Food Chem Toxicol., 85:61-70.

Shim, K.H., J. Hulme, E.H. Maeng, M.K. Kim, and S.S. An, 2014. Analysis of zinc oxide nanoparticles binding proteins in rat blood and brain homogenate. Int. J. Nanomedicine 9 Suppl., 2:217 -24.

Siciliano, M.J., and C.R. Shaw, 1976. Separation and visualization of enzymes on gels. In: Chromatographic and Electrophoretic Techniques. Vol. 2. Zone Electrophoresis. 4th edn, (Ed I Smith), 185-209.

Srividhya, R., R. Gayathri, and P. Kalaiselvi, 2012. Impact of epigallo catechin-3-gallate on acetylcholine-acetylcholine esterase cycle in aged rat brain. Neurochemistry International, 60:517–522.

Subramaniam, H.N., and K. Chaubal, 1990. Evaluation of intracellular lipids by standardized staining with a Sudan black B fraction. Journal of Biochemical and Biophysical Methods, 21:9-16.

Teleanu, D.M., A.G. Niculescu, I.I. Lungu, C.I. Radu, O. Vladâcenco, E. Roza, B. Costăchescu, A.M. Grumezescu, and R.I. Teleanu, 2022. An Overview of Oxidative Stress, Neuroinflammation, and Neurodegenerative Diseases. Int. J. Mol. Sci., 23(11):5938.

Udia, P.M., L.P. Takem, U.F. Ufot, et al., 2016. Insulin and alpha amylase levels in alloxan-induced diabetic rats and the effect of *Rothmannia hispida* (K. Schum) Fagerl leaf extract. J. Phytopharmacol., 5(1):1-5.

Ullah, R., M. Khan, S.A. Shah, K. Saeed, and M.O. Kim, 2019. Natural Antioxidant Anthocyanins-A Hidden Therapeutic Candidate in Metabolic Disorders with Major Focus in Neurodegeneration. Nutrients, 11(6):1195.

Ushio-Fukai, M., D. Ash, S. Nagarkoti, E.J. Belin de Chantemèle, D.J.R. Fulton, and T. Fukai, 2021. Interplay Between Reactive Oxygen/Reactive Nitrogen Species and Metabolism in Vascular Biology and Disease. Antioxid. Redox. Signal., 34(16):1319-1354.

Xiong, J., H. Hu, R. Guo, H. Wang, and H. Jiang, 2021. Mesenchymal Stem Cell Exosomes as a New Strategy for the Treatment of Diabetes Complications. Front Endocrinol (Lausanne)., 12:646233.

Xu, F., J. Mu, Y. Teng, X. Zhang, K. Sundaram, M.K. Sriwastva, A. Kumar, C. Lei, L. Zhang, Q.M. Liu, J. Yan, C.J. McClain, M.L. Merchant, and H.G. Zhang, 2022. Restoring Oat Nanoparticles Mediated Brain Memory Function of Mice Fed Alcohol by Sorting Inflammatory Dectin-1 Complex Into Microglial Exosomes. Small, 18(6):e2105385.

Xu, F., J. Xu, X. Xiong, and Y. Deng, 2019. Salidroside inhibits MAPK, NF-κB, and STAT3 pathways in psoriasis-associated oxidative stress via SIRT1 activation. Redox Rep., 24(1):70-74.

Xu, L., A. Shao, Y. Zhao, Z. Wang, C. Zhang, Y. Sun, J. Deng, and L.L. Chou, 2015. Neurotoxicity of Silver Nanoparticles in Rat Brain After Intragastric Exposure. J Nanosci Nanotechnol., 15(6):4215-23.

Yeh, W.J., S.M. Hsia, W.H. Lee, and C.H. Wu, 2017. Polyphenols with antiglycation activity and mechanisms of action: A review of recent findings. J. Food Drug Anal., 25(1):84-92.